Modal Noise Mitigation in 850 nm VCSEL-based Transmission Systems over Single-Mode Fiber

Jacopo Nanni, Simone Rusticelli, Carlos Viana,
Jean-Luc Polleux, Catherine Algani, Federico Perini, Giovanni Tartarini

***Abstract*—Various short-range optical connections, transmitting either high-bit-rate digital signals, or Radio Frequency (RF) analog signals can exploit 850 nm Vertical Cavity Surface Emitting Lasers (VCSELs) as optical source together with the standard single mode fiber as optical channel. This solution presents attractive features in terms of reduced cost and energy consumption. However, bandwidth reduction due to intermodal dispersion and undesired fluctuations of the received signal due to modal noise are present in this case. Such effects are studied theoretically and experimentally, and a cost effective solution is proposed to reduce their impact. Hence, connections with Standard Single Mode Fiber (SSMF) length up to 300 m with 3 dB bandwidth of 2500 MHz is demonstrated whilst the modal noise is reduced to a standard deviation of less than 2 dB.**

***Index Terms*—radio over fiber, radio astronomy, home area network, RF gain, VCSEL.**

I. Introduction

The employment of vertical cavity lasers (VCSELs) operating at 850 nm to realize optical transmission systems presents attractive aspects. This because VCSELs are inherently low cost components, exhibiting low levels of current consumption when compared to other types of semiconductor lasers [1].

VCSELs operating at 850 nm are usually employed together with Multi Mode Fibers (MMFs), e.g., to realize optical links within data centers [2] or to transmit 60 GHz wireless signals in home-area-networks [3].

Nevertheless, the combined adoption of 850 nm VCSELs for transmission over ITU-T G.652 Standard Single Mode Fibers (SSMFs), constitutes an important investigation topic, because SSMFs present lower cost per meter and lower sensitivity to bends than MMFs. In addition to this, many offices and private houses are already equipped with a SSMF infrastructure at the building stage, in view of the foreseeable demand from high bandwidth services in the near future [4].

However, key to successful transmission is addressing some of the potential impairments. With respect to other lasers, e.g., Distributed Feed Back (DFB) lasers operating in the second ($\lambda \simeq 1310$ nm) and third ($\lambda \simeq 1550$ nm) optical windows, VCSELs emit much lower optical power, as well as multiple spectral lines with larger linewidths. At the same time, SSMFs exhibit a multimode behavior at $\lambda \simeq 850$ nm. For these reasons the use of VCSEL-based transmission systems on SSMFs cannot cover long distances. Despite this, their potential interest is not compromised, because many new applicative scenarios require only short distances to be covered. Such systems employ a digital modulation of VCSELs for the realization of high-bit-rate connections over distances ranging from a few tens to a few hundreds of meter [5].

Moreover, the analog modulation of the VCSEL by an RF signal allows a transparent and robust transmission to remotely-located processing units through the Radio over Fiber (RoF) technology. This becomes very useful in applications related to multivariate fields, such as measurement, monitoring, meteorology, defense, telecommunications and radio astronomy [6], [7].

However, even within short-range links, the different fiber modes propagating in the SSMF exhibit different group velocities. This causes the phenomenon of intermodal dispersion, leading to a bandwidth limitation in case of analog RoF systems, or to a Bit Error Rate (BER) or Error Vector Magnitude (EVM) increase in case of digital optical links [8], [9].

Furthermore, the different fiber modes feature time varying mutual phase differences, since their propagation constants are differently affected by changes of external quantities like temperature. This characteristic gives rise to the phenomenon of modal noise, which results in undesired fluctuating behaviors of the received power [10].

For digital or analog modulation of the VCSEL, key to the evaluation of the transmission quality is the frequency response of the whole link, which can be represented by the RF gain $G = 10\log_{10}(P_{RF,out}/P_{RF,in})$ where $P_{RF,in}$ and $P_{RF,out}$ are respectively the input and the output RF power of the link. The undesired fluctuations due to modal noise can then be evaluated considering either the variance σ_G^2 or the standard deviation σ_G of G [11].

Previous studies of optical links based on SSMFs utilizing 850 nm VCSELs as optical sources, propose different methods for the mitigation of the above mentioned impairments [12]–[16].

The problem has been addressed in [12], where a low frequency superposition technique is proposed to reduce the coherence of the optical source and consequently modal noise. A drawback of this proposal is that it adds complexity to the system, since the additional RF generator should be tuned each

J. Nanni and G.Tartarini are with the Dipartimento dell'Energia Elettrica e dell'Informazione "Guglielmo Marconi" Università di Bologna, 40136 Bologna, Italy (e-mail: jacopo.nanni3@unibo.it; giovanni.tartarini@unibo.it).

J.L.Polleux and C.Viana are with Université Paris-Est, ESYCOM (EA2552), ESIEE Paris, UPEM, Le Cnam, 93162 Noisy-le-Grand, France (e-mail: jean-luc.polleux@esiee.fr; carlos.viana@esiee.fr).

C.Algani is with Le Cnam, ESYCOM (EA2552), 75003 Paris, France (e-mail: catherine.algani@cnam.fr).

F.Perini and S.Rusticelli are with Institute of Radio Astronomy, National Institute for Astrophysics, Via Fiorentina 3513, 40059 Medicina, Italy (e-mail: f.perini@ira.inaf.it;s.rusticelli@ira.inaf.it).

time depending on the link length and/or the RF frequency transmitted.

With the aim to reduce the intermodal dispersion, in [13], a special ITU-T G.652 compliant graded index fiber is utilized, while in [14], [15] different types of fiber mode filters are realized. However, these solutions are based on ad hoc components, and their adoption would determine an increase in complexity and system cost.

With the same objective, in [16], fiber loops of short diameter are inserted and used as a fiber mode filtering at the beginning and at the end of the fiber span.

This method is simple so infers lower cost, but repeatability may be an issue considering the deployment of such systems. In addition, effectiveness of the solution have been addressed in terms of system average bandwidth, without considering the impact of modal noise.

The insertion of a short span of $5\,\mu$m-core fiber, which is truly single mode at 850 nm ($SMF_{5\mu m}$) at the end of the SSMF strand is finally proposed in [5]. This simple solution, however has a detrimental impact as modal noise increases. This has been shown in [17], where the impact of modal noise in the structure proposed in [5] has been experimentally studied.

In this paper, a theoretical and experimental study is performed on the impact of modal noise in 850 nm VCSEL-based transmission links based on SSMF. To show its characteristics, the analysis includes systems with strong discontinuities, like the one proposed in [5], to which forced temperature variations are introduced. As a result of the investigation performed, a simple and repeatable solution is presented to reduce the system impairments. Instead of inserting a $SMF_{5\mu m}$ between the SSMF strand and the photodiode, as proposed in [5], our solution proposes the insertion of the $SMF_{5\mu m}$ between the VCSEL and the SSMF strand.

Note that the optical channel configuration that results from the proposal illustrated in this work is similar to the structures proposed in [18], [19]. However, the context of these works, both operating at $\lambda = 1550$ nm, is different, as well as their investigation. Indeed, in [18] an increase of the bandwidth-distance product is pursued, while in [19], the study of the structure is performed for sensor applications. In both cases the problem of modal noise is not investigated.

The paper is organized as follows. In the next section a theoretical model will be developed to illustrate the expected behavior of VCSEL-based transmission systems in terms of modal noise and intermodal dispersion.

In Section III, experimental results are presented, which will show the advantages of the proposed solution in terms of reduction of such impairments in short-range links. Finally, conclusions will be drawn.

II. Mathematical model

A. Definition of the problem

The electromagnetic problem consists of modeling the multimodal propagation in a strand of SSMF operating at 850 nm. To give a clearer illustration of the physical phenomena involved some approximations are made. First of all, for a SSMF the resulting value of the normalized frequency is between $v \in [3.2, 4.0]$. Therefore, it is assumed that the number N_m of fiber modes propagating in the SSMF is $N_m = 2$, namely the first (LP_{01}) and the second mode (LP_{11}), since the third one (LP_{21}), when present, is just above cutoff. The assumption is supported by the tolerance values of the mode field diameter given by the ITU G.652 standard for $\lambda = 1310$ nm. The nominal range is $[8.6 - 9.5]\,\mu m$ with a tolerance of $\pm 0.6\,\mu m$, hence the mode field diameter is extended by $[8 - 10.1]\,\mu m$. With a typical numerical aperture of 0.12, the number of propagating modes at the operation wavelength $\lambda_{op} = 850$ nm can be computed.

A second approximation consists in considering the N_L lines of the VCSEL emission spectrum as independent sources emitting at different wavelengths separated by a few tenths of nm one from the other. This is justified by the fact that the mode partition noise among the different lines of the VCSEL emission spectrum is typically negligible with respect to the fluctuations caused by modal noise [20], [21]. The gain variance σ_G^2 will then be computed as a weighted sum of the variances corresponding to each line, which will be assumed equal ($\sigma_{G,k}^2 = \sigma_{G,line}^2, \quad k = 1, ..., N_L$), according to:

$$\sigma_G^2 = \sum_{k=1}^{N_L} p_k^2 \sigma_{G,k}^2 = \sigma_{G,line}^2 \sum_{k=1}^{N_L} p_k^2 \tag{1}$$

In (1) the coefficient p_k represents the percentage of power carried by the k-th line, and then $\sum_{k=1}^{N_L} p_k = 1$ [22].

The average value of G will instead coincide with the average RF gain computed considering each line separately:

$$\langle G \rangle_k = \left\langle 10 \log_{10} \left[\frac{p_k^2 P_{RF,out}}{p_k^2 P_{RF,in}} \right] \right\rangle = \langle G \rangle \qquad k = 1, ..., N_L \tag{2}$$

where $\langle (\cdot) \rangle$ means that a time average of the quantity $(\cdot)$ is computed.

To determine the expression of $\sigma_{G,line}$ it is necessary to start from the expression of the field at the output section of the SSMF strand with length L_1 due to the generic line of the spectrum emitted by the VCSEL, which can be written as:

$$\begin{aligned} \bar{E}(t, L_1) = \sum_{i=1}^{N_m} A_i \bar{e}_i(x, y) e^{j(2\pi f_0 t - \beta_i(t) L_1)} \cdot \\ \cdot \sqrt{1 + m_I \cos[2\pi f_{RF}(t - \tau_i L_1)]} \cdot \\ \cdot e^{-j \frac{K_I I_{0\,in,RF}}{f_{RF}} \sin[2\pi f_{RF}(t - \tau_i L_1)]} \end{aligned} \tag{3}$$

where f_0 is the optical carrier's frequency, $\bar{e}_i(x, y)$ is the normalized field of the i-th fiber mode, A_i is its amplitude (assumed real), which depends on the excitation field considered, while $\beta_i(t)$ is its phase constant. The quantity $\beta_i(t)$ is assumed as time-varying, due to changes in environmental quantities, like temperature. The group delay per unit length of the i-th fiber mode is indicated as τ_i.

Note that all the quantities listed above are different for the different lines of the VCSEL emission spectrum. For the k-th line it should consequently be necessary to write respectively $f_{0,k}$, $\bar{e}_{i,k}(x, y)$, $A_{i,k}$, $\beta_{i,k}(t)$, $\tau_{i,k}$. However, as

shown above, the expressions of G and σ_G can be determined from the computation of the correspondent quantities referred to a generic single line. Once the line is chosen, it will then be the only one considered in the derivation. The subscript k can then be omitted for the sake of formal simplicity.

Still referring to (3), f_{RF} is the frequency of the modulating RF signal, while the ratio $\frac{K_f I_{0\,in,RF}}{f_{RF}}$ can be regarded as the phase modulation index of the optical wave determined by the frequency chirp of the laser, and will be indicated as m_P. Within m_P, K_f is the laser adiabatic chirp factor, while $I_{0\,in,RF}$ is the amplitude of the modulating RF current $i_{in,RF}(t) = I_{0\,in,RF}\cos(2\pi f_{RF} t)$.

The sum $\sum_{i=1}^{N_m} A_i^2$ is proportional to the term $\eta_0(I_{bias} - I_{th})$, where η_0 is the current-power conversion efficiency of the laser at DC, while I_{bias} and I_{th} are respectively the laser bias and threshold currents. With m_I the optical modulation index is indicated, defined as $m_I = (\eta_{RF} I_{0\,in,RF})/[\eta_0(I_{bias} - I_{th})]$, where η_{RF} is the current-power conversion efficiency of the laser at frequency f_{RF}.

Note that the LP_{01} and the LP_{11} fiber modes are constituted respectively by a group of two and a group four rigorously computed fiber modes (RCFM). The first group of RCFM contains the HE_{11} in its two polarizations, while the second one contains the TE_{01} and TM_{01} plus the HE_{21} in its two polarizations.

In (3), a complete coupling is assumed within the two mode groups, while the coupling between them is assumed to be negligible [23]. This hypothesis is justified by the fact that a length $L_1 \leq 300$ m is considered for the SSMF fiber span and that the environmental perturbations consist in temperature variations slower than 1 K/min. Different perturbations, for example a varying mechanical stress, which can force a strong coupling between LP_{01} and LP_{11} fiber modes even at short lengths, are out of the scope of this work and are consequently not considered.

B. Computation of the output current and evaluation of its behavior

After propagating inside the $SMF_{5\mu m}$ patch of length L_2 the field is expressed by:

$$\begin{aligned}
&\bar{E}(t, L_1 + L_2) = \\
&= \bar{e}_{1_{SMF_{5\mu m}}}(x,y) e^{j(2\pi f_0 t - \beta_{1_{SMF_{5\mu m}}} L_2)} \cdot \\
&\cdot \sum_{i=1}^{N_m} A_i a_{i1} e^{-j[\beta_i(t) L_1]} \cdot \\
&\cdot \sqrt{1 + m_I \cos[2\pi f_{RF}(t - \tau_i L_1 - \tau_{1_{SMF_{5\mu m}}} L_2)]} \cdot \\
&\cdot e^{-j m_p \sin[2\pi f_{RF}(t - \tau_i L_1 - \tau_{1_{SMF_{5\mu m}}} L_2)]}
\end{aligned} \tag{4}$$

where $\bar{e}_{1_{SMF_{5\mu m}}}(x,y)$ is the normalized field of the LP_{01} mode propagating in the $SMF_{5\mu m}$, while $\beta_{1_{SMF_{5\mu m}}}(t)$ is its phase constant. The quantity

$$a_{i1} = \int_{S_{SMF_{5\mu m}}} \bar{e}_i \cdot \bar{e}^*_{1_{SMF_{5\mu m}}} dS \tag{5}$$

where $S_{SMF_{5\mu m}}$ is the cross section of the $SMF_{5\mu m}$ fiber, represents the overlap integral between the i-th mode of the SSMF and the LP_{01} mode of the $SMF_{5\mu m}$. Note that due to the shapes of the fields of the fiber modes considered, in case of ideal connection it should be $a_{11} \neq 0$ and $a_{21} = 0$. However, due to imperfections in the connection, for example the presence of connector misalignments, a value $a_{21} \neq 0$ has to be taken into account. The detected current is proportional to the optical power received on the photodiode (PD) surface S_{PD} (a responsivity $\mathcal{R} = 1$ is assumed). Putting $L = L_1 + L_2$, it is then:

$$i_{out}(t) = \int_{S_{PD}} |\bar{E}(t, L)|^2 dS \tag{6}$$

Computing the integral at the second side of (6), the expression of the output current becomes:

$$\begin{aligned}
&i_{out}(t) = \\
&= \sum_{i=1}^{N_m} A_i^2 a_{i1}^2 b_{11_{SMF_{5\mu m}}} \\
&\cdot (1 + m_I \cos(2\pi f_{RF}(t - \tau_i L_1 - \tau_{1_{SMF_{5\mu m}}} L_2))) \\
&+ 2 A_1 A_2 a_{11} a_{21} b_{11_{SMF_{5\mu m}}} \\
&\cdot [1 + m_I \cos(2\pi f_{RF} \Delta\tau) \cos(2\pi f_{RF}(t - \bar{\tau})] \\
&\cdot \Big[\cos(\Delta\beta(t)) \cos(x \cos(2\pi f_{RF}(t - \bar{\tau}))) \\
&+ \sin(\Delta\beta(t)) \sin(x \cos(2\pi f_{RF}(t - \bar{\tau}))) \Big]
\end{aligned} \tag{7}$$

where the following parameters are defined:

$$b_{11_{SMF_{5\mu m}}} = \int_{S_{PD}} |\bar{e}_{1_{SMF_{5\mu m}}}|^2 dS \tag{8}$$

$$\Delta\beta(t) = (\beta_2(t) - \beta_1(t)) L_1 \tag{9}$$

$$\Delta\tau = \frac{(\tau_1 - \tau_2) L_1}{2} \tag{10}$$

$$x = 2 \cdot m_p \sin(2\pi f_{RF} \Delta\tau) \tag{11}$$

$$\bar{\tau} = \frac{(\tau_1 + \tau_2) L_1}{2} + \tau_{1_{SMF_{5\mu m}}} L_2 \tag{12}$$

With reference to the last term within square brackets at the second side of (7), the relation $e^{ju\cos(v)} = \sum_{n=-\infty}^{+\infty} j^n J_n(u) e^{jnv}$ is exploited, where $J_n(u)$ is the Bessel function of first kind and order n, and where $u = x$ and $v = \cos(2\pi f_{RF}(t - \bar{\tau}))$. Considering only the RF components of $i_{out}(t, L)$, it is possible to write the following expression:

$$\begin{aligned}
i_{out,RF}(t) =& [\mathcal{A}_c + \mathcal{B}_c(t)] \cos(\omega_{RF} t) \\
&+ [\mathcal{A}_s + \mathcal{B}_s(t)] \sin(\omega_{RF} t) \\
=& \Re\{\tilde{I}_{out,RF}(t) e^{j\omega_{RF} t}\}
\end{aligned} \tag{13}$$

where

$$\tilde{I}_{out,RF}(t) = [\mathcal{A}_c + \mathcal{B}_c(t)] - j[\mathcal{A}_s + \mathcal{B}_s(t)] \tag{14}$$

is the complex envelope of the bandpass signal, while

$$\mathcal{A}_c = \sum_{i=1}^{N_m} m_I A_i^2 a_{i1}^2 b_{11_{SMF_{5\mu m}}} \cdot \cos[2\pi f_{RF}(\tau_i L_1 + \tau_{1,SMF_{5\mu m}} L_2)] \quad (15)$$

$$\mathcal{A}_s = \sum_{i=1}^{N_m} m_I A_i^2 a_{i1}^2 b_{11_{SMF_{5\mu m}}} \cdot \sin[2\pi f_{RF}(\tau_i L_1 + \tau_{1,SMF_{5\mu m}} L_2)] \quad (16)$$

$$\mathcal{B}_c(t) = 2A_1 A_2 a_{11} a_{21} b_{11_{SMF_{5\mu m}}} C(t) \cos(2\pi f_{RF} \bar{\tau}) \quad (17)$$

$$\mathcal{B}_s(t) = 2A_1 A_2 a_{11} a_{21} b_{11_{SMF_{5\mu m}}} C(t) \sin(2\pi f_{RF} \bar{\tau}) \quad (18)$$

and where:

$$C(t) = m_I \cos(2\pi f_{RF} \Delta\tau) J_0(x) \times \times \cos(\Delta\beta(t) L_1) + 2J_1(x) \sin(\Delta\beta(t) L_1) \quad (19)$$

In the case where there is no $SMF_{5\mu m}$ at the end of the SSMF span, $i_{out,RF}(t)$ assumes the same formal aspect as in (13) the only difference being that that in (15) and (16) the term $a_{i1}^2 b_{11_{SMF_{5\mu m}}}$ must be replaced by b_{ii} and in (17) and (18) the term $a_{11} a_{21} b_{11_{SMF_{5\mu m}}}$ must be replaced by b_{12}, where

$$b_{ij} = \int_{S_{PD}} \bar{e}_i \cdot \bar{e}_j^* dS \qquad i,j = 1,2 \quad (20)$$

It can be noted that, due to the orthogonality of the SSMF modes, in case of a photodiode with infinite surface S_{PD} it should be $b_{11}, b_{22} = 1$ and $b_{12} = 0$. However, $b_{12} \neq 0$ has to be taken into account because of the finite dimensions of a realistic photodiode.

The quantities $\mathcal{B}_c(t)$ and $\mathcal{B}_s(t)$ given by (17) and (18) represent the time dependent contributions due to the temperature fluctuations, while $\mathcal{A}_c$ and $\mathcal{A}_s$ remain constant over time. The envelope of $i_{out,RF}(t)$ is given by

$$|\tilde{I}_{out,RF}(t)| = \sqrt{(\mathcal{A}_c + \mathcal{B}_c(t))^2 + (\mathcal{A}_s + \mathcal{B}_s(t))^2} \quad (21)$$

Since the time dependent terms have zero mean, the magnitude of the mean of the RF current received can be written as follows:

$$\mu_{RF} = \left| \left\langle \tilde{I}_{out,RF}(t) \right\rangle \right| = \sqrt{\mathcal{A}_c^2 + \mathcal{A}_s^2} \quad (22)$$

The link RF gain G and its average value $\langle G \rangle$ assume respectively the form:

$$G = 10 \log_{10} \left[\frac{|\tilde{I}_{out,RF}(t)|^2}{|I_{0\,in,RF}|^2} \right] \quad (23)$$

$$\langle G \rangle = 10 \log_{10} \left[\frac{\mu_{RF}^2}{|I_{0\,in,RF}|^2} \right] \quad (24)$$

and the resulting expression of $\sigma_{G,line}$ is therefore given by:

$$\sigma_{G,line} = \sqrt{\left\langle \left\{ 10 \log_{10} \left[\frac{|\tilde{I}_{out,RF}(t)|^2}{\mu_{RF}^2} \right] \right\}^2 \right\rangle} \quad (25)$$

The expression given by (25) can be always utilized. In cases when the following relation holds:

$$|\tilde{I}_{out,RF}(t)| \simeq \sqrt{\mathcal{A}_c^2 + \mathcal{A}_s^2} + + \frac{\mathcal{A}_c}{\sqrt{\mathcal{A}_c^2 + \mathcal{A}_s^2}} \mathcal{B}_c(t) + \frac{\mathcal{A}_s}{\sqrt{\mathcal{A}_s^2 + \mathcal{A}_s^2}} \mathcal{B}_s(t) = = \mu_{RF} + \Delta I_{out,RF} \quad (26)$$

a more treatable expression can be written for $\sigma_{G,line}$. Indeed, exploiting the relationship $20 \log_{10}(1+x) \simeq \frac{20}{\log_e(10)} x$, for $x << 1$, it becomes:

$$\sigma_{G,line} \simeq \frac{20}{\log_e(10)} \frac{\sqrt{\left\langle \Delta I_{out,RF}^2 \right\rangle}}{\mu_{RF}} = = \frac{20}{\log_e(10)} \frac{\sigma_{RF}}{\mu_{RF}} \quad (27)$$

with σ_{RF} representing the standard deviation of $\tilde{I}_{out,RF}$. When the condition given by (26) is not valid, it is necessary to compute $\sigma_{G,line}$ through (25). This happens for example if the LP_{01} and the LP_{11} fiber modes have almost the same weight and the frequency considered is such that $2\pi f_{RF} \Delta\tau$ is an odd integer of $\pi/2$, in which case μ_{RF} tends to zero. Equation (27) is anyway useful because it allows to qualitatively describe some behaviors of $\sigma_{G,line}$.

Indeed, in the vicinity of the frequencies mentioned above, μ_{RF}, which is at the denominator, diminishes its value. At the same time, it can be observed that σ_{RF}, which is at the numerator, depends (see (27) and (26)) on the standard deviation of the terms $\mathcal{B}_c(t)$ and $\mathcal{B}_s(t)$, which in turn (see (17) and (18)) depend on the standard deviation of the term $C(t)$ given by (19). The expression of $C(t)$ is composed by the sum of two addends. The first depends on $\cos(2\pi f_{RF} \Delta\tau)$ and tends to zero when the frequency f_{RF} is such that $2\pi f_{RF} \Delta\tau$ tends to be an odd integer of $\pi/2$. The second addend is proportional to $J_1(x)$, where x, given by (11), is instead proportional to $\sin(2\pi f_{RF} \Delta\tau)$ and tends to a maximum for the same frequencies. The values assumed by x allow typically to put $J_1(x) \sim x/2$, and therefore it can be expected that $\sigma_{G,line}$ due to modal noise exhibits high values in the vicinity of the frequencies f_{RF} where μ_{RF} tends to a minimum.

C. Numerical results

The model developed has been used to qualitatively predict the performance of VCSEL-based SSMF transmission links with different configurations of the optical channel. Table I lists the values of the electrical and optical quantities of the modeled system, which are the characteristics of the real system on which the experimental activity was subsequently performed. In particular, since the emission spectrum of the VCSEL utilized presents two lines of approximately the same weight which prevail over the others by at least 6 dB, it results in:

$$\sigma_G \simeq \frac{1}{\sqrt{2}} \sigma_{G,line} \quad (28)$$

The first analysis has been performed on the characteristics of a link where a short span (3 m) of $SMF_{5\mu m}$ is placed

TABLE I
SOME CHARACTERISTIC QUANTITIES OF THE COMPONENTS OF THE VCSEL-BASED TRANSMISSION SYSTEM ANALYZED

$VCSEL$ parameters:	
· I_{th}	0.8 mA
· η_0	0.1 mW/mA
· η_{RF}	0.1 mW/mA
· K_f	0.6 GHz/mA
· $p_1 \simeq p_2$	1/2
· N_L	2
PIN parameters:	
· $\mathcal{R}$	1 mA/mW
· B_{PIN}	2.5 GHz
$I_{0\,in,RF}$	1.2 mA
I_{bias}	4 mA
$\tau_2 - \tau_1$	2.3 ps/m

between SSMF and PD, with SSMF strand length $L_1 = 300$ m.

The $SMF_{5\mu m}$ span, which exhibits a single mode behavior at $\lambda = 850$ nm, performs an output filtering operation. Indeed, this solution has been shown to determine an increase of the passband with respect to the case where only a SSMF strand is utilized, leading to a BER reduction of digital optical links [5].

Fig. 1 reports modeled results which compare the performance of the optical link having the $SMF_{5\mu m}$ at the SSMF end section, to when only the SSMF is used (without $SMF_{5\mu m}$).

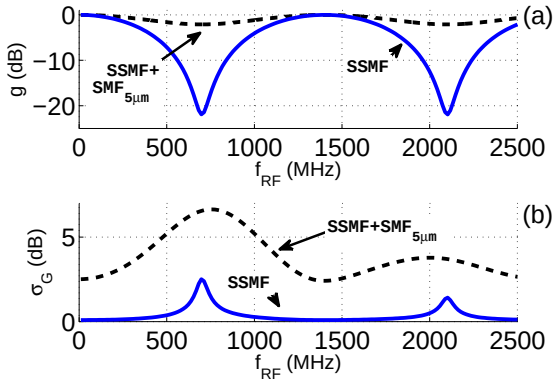

Fig. 1. Comparison of simulated results for a transmission link with SSMF length $L_1 = 300$ m in case of presence and in case of absence of $SMF_{5\mu m}$ patch between SSMF and PD. The bandwidth improvement due to the $SMF_{5\mu m}$ employment can be noticed in (a) while the increase of the standard deviation σ_G of the fluctuations of G due to modal noise is shown in (b). The parameters values utilized in the simulation program are: $m_I = 0.375, A_1^2 = 0.55, A_2^2 = 0.45, a_{11}^2 = 0.9, a_{12}^2 = 0.065, b_{11} = 0.985, b_{22} = 0.985, b_{12} = 0.015$.

The simulations confirm that the insertion of $SMF_{5\mu m}$ at the output section of the SSMF improves the available bandwidth. Fig. 1 (a) shows the behavior of the normalized gain $g = \langle G \rangle - \langle G \rangle |_{max}$. It can be noticed that the difference Δg between the maximum and the minimum values of g is largely reduced by the introduction of the $SMF_{5\mu m}$ patch with respect to the case when only the SSMF is present. It is

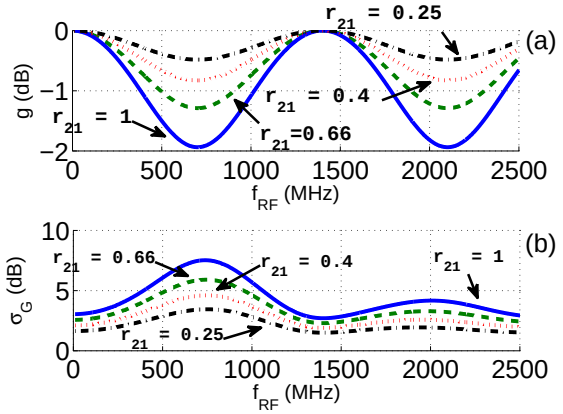

Fig. 2. Behavior of g (a) and σ_G (b) as a function of the RF modulating frequency as function of the parameter $r_{21} = (A_2/A_1)^2$. A reduction in both Δg and σ_G can be noticed due to the reduction of A_2 with respect to A_1. The transmission link considered is the one with SSMF length $L_1 = 300$ m in case of presence of $SMF_{5\mu m}$ patch between SSMF and PD.

however important to observe, that, as reported in Fig. 1 (b), the model predicts an increase of the maximum value $\sigma_G|_{max}$ of σ_G in the structure proposed in [5], with respect to the case of the SSMF span alone. Moreover, in the vicinity of $\sigma_G|_{max}$ an enlargement of the bandwidth where the values of σ_G are relatively high results in the case when the $SMF_{5\mu m}$ is present.

The expression of $\sigma_{G,line}$ given by (27), where μ_{RF} is present at denominator, suggests that a reduction of the amplitude A_2 of the LP_{11} fiber mode would diminish the impact of modal noise. In fact, reducing the degree of destructive interference at the detection stage, the presence of the minima of μ_{RF} is also reduced, mitigating the effect of modal noise.

This is the main contribution of our proposal to inserting a $SMF_{5\mu m}$ patch before (and not after) the SSMF strand. The simulated results reported in Fig. 2 show the expected behavior of the transmission link in terms of g and σ_G when the value of A_2 is gradually reduced with respect to A_1. The transmission link features a SSMF length $L_1 = 300$ m and a $SMF_{5\mu m}$ patch between SSMF and PD, and all the other parameters are the same as in Fig. 1. Positive effects are observed in the behavior of g (Fig. 2 (a)), since the value of Δg decreases when A_2 is reduced with respect to A_1.

In addition to this, Fig. 2 (b) suggests that important reductions of σ_G can be expected when the relative weight of the LP_{11} fiber mode is reduced with respect to the LP_{01}. In this way we expect that the large reduction of A_2 leads to a low impact of the terms related to modal noise given by (17) and by (18), in which case the quantity b_{12} expressed in (20) which is expectedly small as well, has to be inserted. In the next section an experimental analysis will be performed on VCSEL-based SSMF transmission links to confirm the previsions of the mathematical model and propose this solution to reduce the impact of modal noise in these systems.

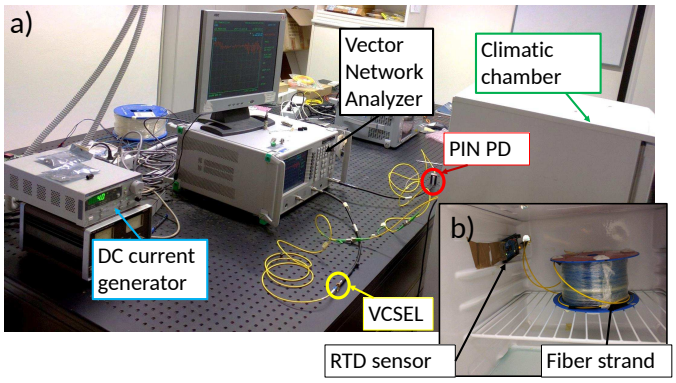

Fig. 3. Experimental setup utilized evidencing its portions placed (a) outside and (b) inside the climatic chamber.

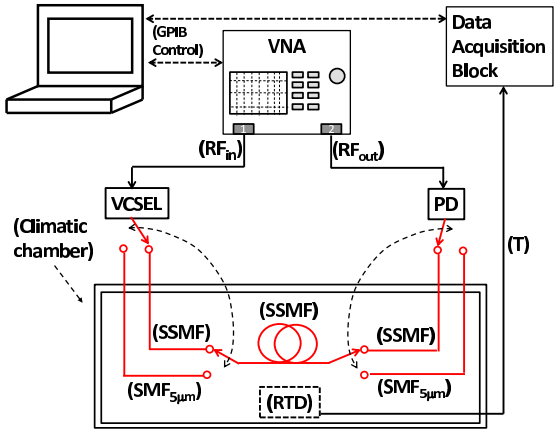

Fig. 4. Functional scheme of the experimental setup.

III. Experimental Results and Discussion

A. Experimental setup

The experimental setup utilized to characterize VCSEL-based transmission links based on SSMFs is shown in Fig. 3, while its functional scheme is drawn in Fig. 4.

A directly modulated 10 Gbps VCSEL (Optowell TP85-LCP1H) emitted the optical signal into a channel constituted by a ITU-T G.652 SSMF strand. Short spans (3 m) of Thorlabs 780HP $SMF_{5\mu m}$ could be added before its input and/or after its output section. The optical receiver was constituted by a PIN PD (Optowell RP85-LCT0N) followed by a RF matching circuit. As preliminary measurement, the frequency response (i.e. the RF gain) of the link was measured utilizing as optical channel two meter of 50 μm core MMF. In this way, the RF gain caused by the frequency responses of transmitter and receiver could be determined. This measurement was utilized to infer the influence on the behavior of $\langle G \rangle$ and g. These are determined by the only optical channel when it is consisting of various combinations of SSMF and $SMF_{5\mu m}$. The link exhibited a bandwidth of about 2.5 GHz. A Vectorial Network Analyzer (VNA) was then used to generate and receive different frequencies in the bandwidth $B = [10$ MHz, 2.5 GHz] through port 1 and port 2, respectively.

As mentioned in subsection II-C, short spans of $SMF_{5\mu m}$ were utilized in addition to the SSMF strands, because of their true single mode behavior at $\lambda = 850$ nm. To emulate possible conditions causing modal noise, a temperature stress was produced. This was done by the insertion of the G.652 strand inside a climatic chamber, controlled and monitored by a Resistor Temperature Detector (RTD) sensor connected to a digital data acquisition block (see again Fig. 4). All the measurement instruments were then connected to a PC through GPIB cables and controlled and monitored with a Labview® Graphical User Interface. Using the VNA, the measurement of the behavior of G versus time due to temperature variations was performed in a time span of few hours, with a sampling time of 6 seconds. The quantities $\langle G \rangle$ and σ_G could be determined from the values of $G(t)$.

B. Experimental results

Different configurations of the optical channel were considered to investigate the behavior of modal noise and take appropriate countermeasures. The first analysis regarded the effect of the insertion, (see Fig. 4), of an $SMF_{5\mu m}$ span between SSMF and PD. A passband increase can be observed in Fig. 5 (a), which compares the behaviors of g in the two cases, with reference to a SSMF strand of length $L_1 = 300$ m. The value of Δg has been measured to be about 6 dB in the frequency range $B = [10$ MHz, 2.5 GHz], while the same quantity showed a much higher value of about 34 dB in the case when only the SSMF is used.

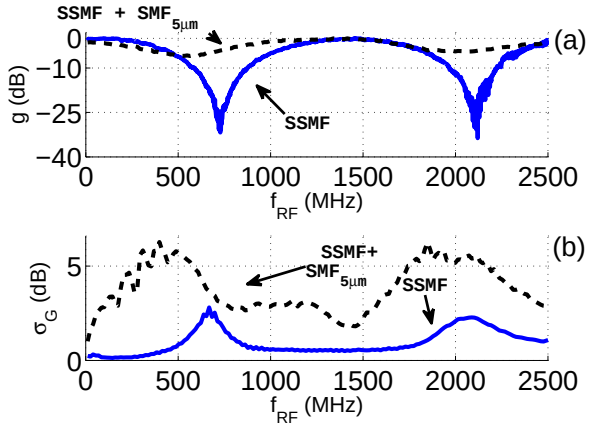

Fig. 5. Behaviors of g (a) and σ_G (b) versus frequency of two VCSEL based transmission links utilizing 300 m of SSMF, respectively with and without $SMF_{5\mu m}$ at the end of the SSMF span. The curves reported in (b) coincide with the curves representing the standard deviation σ_{NF} of the noise figure NF of the links considered.

However, as expected from the numerical results presented in subsection II-C, this solution also brings about an undesired increase of modal noise. Fig. 5 (b) allows to observe the increase of σ_G, whose maximum value $\sigma_G|_{max}$ is about 6 dB, which is more than 3 dB larger than the case when only 300 m of SSMF was used. Note that, in agreement with the modeled results of the previous Section, in the vicinity of $\sigma_G|_{max}$ an enlargement of the bandwidth where the values of σ_G are relatively high is observed in the case when the

$SMF_{5\mu m}$ is present, with respect to the case of the SSMF span alone.

Nevertheless, this configuration will be taken as the reference since it emulates the worse performance for VCSEL-based SSMF transmission link in terms of modal noise.

The presence of a truly singlemode fiber at 850 nm between VCSEL and SSMF propagates mostly the LP_{01} fiber mode. Hence a very low weight is assigned to the higher order mode. The effect of this solution can be noticed in Fig. 6.

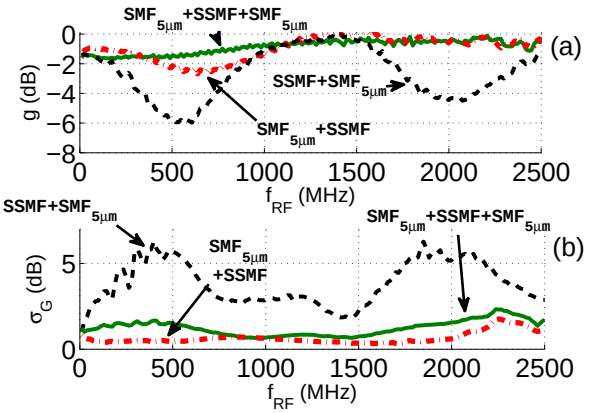

Fig. 6. Behaviors of g (a) and σ_G (b) versus frequency of three VCSEL based transmission links utilizing 300 m of SSMF, respectively with a patchcord of $SMF_{5\mu m}$ at the beginning, at the end, and both at the beginning and at the end of the SSMF span. As in Fig. 5 (b), the curves reported in (b) are also representative of the standard deviation σ_{NF} of the noise figure NF of the links considered.

An improvement in terms of the system bandwidth can be noticed in Fig. 6 (a), where it is $\Delta g \simeq 6$ dB in the system described in [5] (SSMF $+SMF_{5\mu m}$) whereas it is $\Delta g \simeq 1.6$ dB when an additional $SMF_{5\mu m}$ patch-cord is placed between the VCSEL and the SSMF strand ($SMF_{5\mu m}$+ SSMF $+SMF_{5\mu m}$). In terms of 3 dB modulation bandwidth, computed taking as a reference $g(0)$, the improvement goes from $B_{3_{dB}} \simeq 380$ MHz to $B_{3_{dB}} \simeq 2500$ MHz.

A noticeable improvement can additionally be observed in Fig. 6 (b), where $\sigma_G|_{max}$ is reduced to less than $2\,dB$ within B. The performance of the structure SSMF $+SMF_{5\mu m}$ has then shown an important improvement with the introduction of the $SMF_{5\mu m}$ patch before the SSMF strand.

With the aim to consider a more realistic condition, in Fig. 6 it has also been reported the behavior of a VCSEL-based transmission link where the $SMF_{5\mu m}$ patch is placed before the SSMF strand of length $L_1 = 300$ m, and no other $SMF_{5\mu m}$ patch is placed after. This configuration shows indeed a slightly higher value of Δg ($\simeq 2$ dB) which anyway leads to the same $B_{3_{dB}} = 2500$ MHz with respect to the case where the $SMF_{5\mu m}$ is placed before and after the SSMF strand. Moreover, $\sigma_G|_{max}$ is further reduced from $\simeq 2.1$ dB to $\simeq 1.8$ dB. Taking also into account the considerations on optical insertion losses specified below, this leads to the conclusion that the only introduction of the $SMF_{5\mu m}$ patch between VCSEL and SSMF gives the best performance in terms of $B_{3_{dB}}$ and $\sigma_G|_{max}$ of short-range VCSEL-based SSMF transmission links. To give an idea of the power penalties caused by the introduction of the $SMF_{5\mu m}$ in the system, the behavior of $\langle G \rangle$ is reported in Fig. 7 (a).

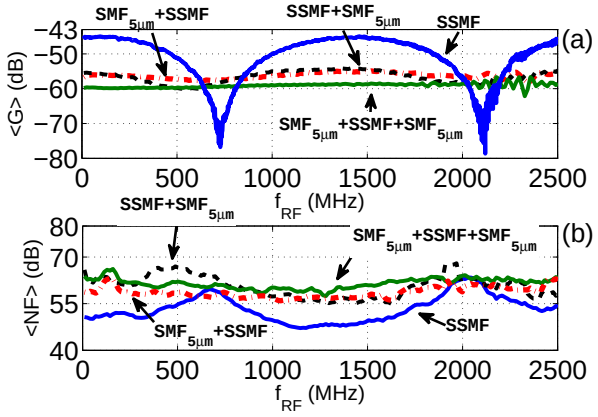

Fig. 7. Behaviors of (a) the average RF gain $\langle G \rangle$ for $L_1 = 300m$ and (b) the noise figure NF, in the four configurations of VCSEL-based transmission links considered in the present work.

The maximum additional RF loss introduced in the configuration where the $SMF_{5\mu m}$ patch is placed both between VCSEL and SSMF and between SSMF and PD can be quantified in about 15 dB, corresponding to 7.5 dB of optical insertion loss. On the contrary, in the case where only one $SMF_{5\mu m}$ patch is utilized (either between VCSEL and SSMF or between SSMF and PD) the two losses are 11-12 dB and 5.5-6 dB respectively.

From the values of $\langle G \rangle$ it is possible to evaluate the average $\langle NF \rangle$ of the noise figure NF in the different cases. This value represents a meaningful quantity in case the VCSEL-based link is utilized for the transmission of RF signals through the RoF technology.

Exploiting the definition (see for example [8]) of NF for RoF links, it is $\langle NF \rangle|_{dB} = N_{out}|_{dB(W/Hz)} - \langle G \rangle|_{dB} - 10\log_{10}(kT)|_{dB(W/Hz)}$, where N_{out} is the available noise output power per unit bandwidth of the system, while $k = 1.38 \cdot 10^{-23}\, Joule/K$ is the Boltzmann constant and $T = 300$ K is the reference temperature. It can be noted that, due to the higher values of $\langle G \rangle$ presented by the configuration where only the SSMF is utilized, the values of $\langle NF \rangle$ are generally smaller than in the other configurations. However, the fluctuations of G due to modal noise cause in turn fluctuations of NF. This leads to standard deviations of the noise figure σ_{NF} represented by the same curves reported in Fig. 5 (b) and Fig. 6 (b). From the observation of both figures, it can be concluded that the solution proposed here ($SMF_{5\mu m}$ patch followed by the SSMF span) is the only one which presents $\sigma_{NF} < 2\,dB$ within the band B.

Keeping in mind applications in the fields of in-building wireless coverage as well as remote radio antennas used for astronomy, further experiments have been performed with lower SSMF lengths. The obtained results can be observed in Fig. 8 which reports the behavior of $\sigma_G|_{max}$ within the bandwidth B when SSMF strands of the same optical fiber with different lengths are utilized.

Starting from the left-hand side, the four histograms report the measured values of $\sigma_G|_{max}$ for $L_1 = 30$ m, 70 m, 100

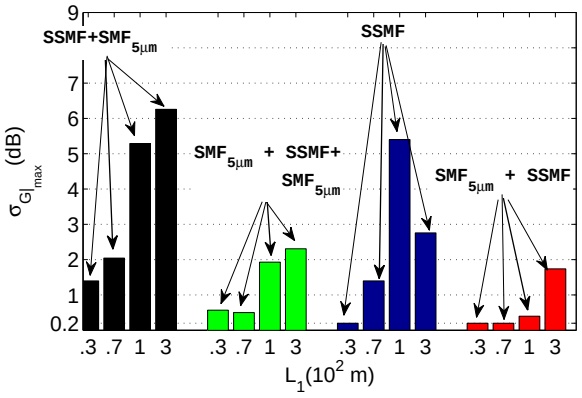

Fig. 8. Behaviors of $\sigma_G|_{max}$ for links of different length L_1 in the four configurations of VCSEL-based transmission links considered in the present work.

m and 300 m, respectively, when the system proposed in [5] is utilized. Proceeding to the right-hand side, the reduction of $\sigma_G|_{max}$ for all the values of L_1 can be observed, when the $SMF_{5\mu m}$ patch is introduced in this system between VCSEL and SSMF. The last two sets of the histograms allow to perform a similar comparison between the cases when the optical channel is constituted by the SSMF strand alone and the case when the $SMF_{5\mu m}$ patch is introduced between the VCSEL and the SSMF strand itself.

Note that in this last case the values of $\sigma_G|_{max}$ are 0.2 dB and 0.3 dB for $L_1 = 70$ m and $L_1 = 100$ m, respectively, which, unlike the case when the initial $SMF_{5\mu m}$ patch is absent, makes the system potentially usable in typical VLBI downlink chains. Indeed, for these applications, fluctuations of G of the order of 0.4 dB are typically required under a temperature stress $\Delta T = 4°$C [24]. Since the values of $\sigma_G|_{max}$ have been measured under a temperature stress $\Delta T \simeq 10°$C, we can conclude that the system proposed here fulfills requirements which are more strict than mentioned above.

IV. Conclusion

In the context of transmission systems adopting 850 nm VCSELs and SSMFs, the effects of the multimodal behavior of the SSMF has an impact simultaneously on the modal interference induced bandwidth reduction and on the generation of modal noise. A mathematical model has been proposed that analyzes the modal impact on such links. It predicts efficiently the behavior of an experimental system using a 10 Gbps VCSEL followed by a SSMF fiber. It is demonstrated, both experimentally and theoretically, that connecting a mode filter such as a $SMF_{5\mu m}$ between the VCSEL and the input of the SSMF fiber, a reduction of both the modal interference and the modal noise impact is obtained. With a SSMF of 300 m length, the bandwidth was increased from $\simeq 250$ MHz to potentially more than 2500 MHz (being limited to this value by the bandwidth of optical transmitter/receiver), while the standard deviation of modal noise was reduced to less than 2 dB. This simple and repeatable solution will thus provide a basis for further improvement in various important contexts. These include the realization of high-bit-rate short-range connections, the transmission of advanced high bandwidth wireless signals in low cost home area networks and local area networks, and the reception of low power signals for astronomy using radio-telescopes.

Acknowledgments

The authors acknowledge the support of prof. Chigo Okonkwo from Technical University of Eindhoven for useful discussions.

References

[1] K. Iga, "Surface-emitting laser-its birth and generation of new optoelectronics field," *IEEE J. Sel. Topics Quantum Electron.*, vol. 6, no. 6, pp. 1201–1215, Nov 2000.

[2] J. A. Tatum *et al.*, "VCSEL-Based Interconnects for Current and Future Data Centers," *J. Lightw. Technol.*, vol. 33, no. 4, pp. 727–732, Feb 2015.

[3] J. Guillory *et al.*, "Comparison between two 60GHz multipoint RoF architectures for the Home Area Network," in *17th European Conf. on Networks and Optical Commun. (NOC)*, Vilanova i la Geltru, Spain, June 2012, pp. 1–5.

[4] M. Fuller, "Weighing MMF vs. SMF in premises applications," *Lightwave*, vol. 3, no. 1, p. 15, Jan 2006.

[5] I. Papakonstantinou, S. Papadopoulos, C. Soos, J. Troska, F. Vasey, and P. Vichoudis, "Modal Dispersion Mitigation in Standard Single-Mode Fibers at 850 nm With Fiber Mode Filters," *IEEE Photonics Technol. Lett.*, vol. 22, no. 20, pp. 1476–1478, Oct 2010.

[6] X. Pang, A. Lebedev, J. J. V. Olmos, I. T. Monroy, M. Beltrn, and R. Llorente, "Performance evaluation for DFB and VCSEL-based 60 GHz radio-over-fiber system," in *17th Int. Conf. Optical Network Design and Modeling (ONDM)*, Brest, France, April 2013, pp. 252–256.

[7] R. Beresford, "ASKAP photonic requirements," in *Int. topical meeting on Microwave Photonics/Asia-Pacific Microwave Photonics (MWP/APMP)*, Gold Coast, Australia, Sept 2008, pp. 62–65.

[8] C. H. Cox, *Analog Optical Links: Theory and Practice*, 1st ed. Cambridge Univ. Press, 2004.

[9] G. Keiser, *Optical Fiber Communications*, 4th ed. Mcgraw Hill Book Co, 2010.

[10] R. E. Epworth, "Modal noise causes and cures," *Laser Focus*, vol. 17, no. 9, pp. 109–115, Sept 1981.

[11] D. Visani, G. Tartarini, M. N. Petersen, L. Tarlazzi, and P. Faccin, "Link Design Rules for Cost-Effective Short-Range Radio Over Multimode Fiber Systems," *IEEE Trans. Microw. Theory Techn.*, vol. 58, no. 11, pp. 3144–3153, Nov 2010.

[12] T. Niiho, K. Masuda, H. Sasai, and M. Fuse, "Proposal of RoF transmission system using 850 nm VCSEL and 1.3 μm SMF with low-frequency superposition technique," in *Optical Fiber Commun. Conf./Nat. Fiber Optic Engineers Conf. (OFC/NFOEC)*, Anaheim, CA, USA, March 2006, pp. 503–505.

[13] M. Stach, F. Pomarico, D. Wiedenmann, and R. Michalzik, "High-performance low-cost optical link at 850 nm with optimized standard singlemode fiber and high-speed singlemode VCSEL," in *30th Europ. Conf. Opt. Commun (ECOC)*, Stockholm, Sweden, Sept 2004, pp. 712–713.

[14] Z. Tian, C. Chen, and D. V. Plant, "850-nm VCSEL Transmission Over Standard Single-Mode Fiber Using Fiber Mode Filter," *IEEE Photonics Techn. Lett.*, vol. 24, no. 5, pp. 368–370, March 2012.

[15] T. Shimizu, K. Nakajima, K. Shiraki, N. Hanzawa, and T. Kurashima, "Multi-Band Mode Filter for Shorter Wavelength Region Transmission over Conventional SMF," in *Conf. Optical Fiber Commun./National Fiber Optic Engineers Conf. (OFC/NFOEC)*, San Diego, CA, USA, Feb 2008, pp. 1–3.

[16] D. Vez, S. G. Hunziker, R. Kohler, P. Royo, M. Moser, and W. Bachtold, "850 nm vertical-cavity laser pigtailed to standard singlemode fibre for radio over fibre transmission," *Electr. Lett.*, vol. 40, no. 19, pp. 1210–1211, Sept 2004.

[17] J. Nanni *et al.*, "Modal noise in 850nm VCSEL-based radio over fiber systems for manifold applications," in *Fotonica AEIT Italian Conf. Photonics Technologies*, Turin, Italy, May 2015, pp. 1–4.

[18] Y. Zhao, Y. Jin, and H. Liang, "Investigation on Single-Mode-Multimode-Single-Mode Fiber Structure," in *Sympos. Photonics and Optoelectronics (SOPO)*, Wuhan, China, May 2011, pp. 1–4.
[19] Z. Haas and M. A. Santoro, "A mode-filtering scheme for improvement of the bandwidth-distance product in multimode fiber systems," *J. Lightw. Technol.*, vol. 11, no. 7, pp. 1125–1131, Jul 1993.
[20] K. H. Hahn, M. R. Tan, Y. M. Houng, and S. Y. Wang, "Large area multitransverse-mode VCSELs for modal noise reduction in multimode fibre systems," *Electron. Lett.*, vol. 29, no. 16, pp. 1482–1483, Aug 1993.
[21] P. Coe, *An Investigation of Mode Partitioning in VCSELS*, HP Laboratories, Bristol, UK, 1996.
[22] R. Dandliker, A. Bertholds, and F. Maystre, "How modal noise in multimode fibers depends on source spectrum and fiber dispersion," *J. Lightw. Technol.*, vol. 3, no. 1, pp. 7–12, Feb 1985.
[23] P. Pepeljugoski, S. E. Golowich, A. J. Ritger, P. Kolesar, and A. Risteski, "Modeling and simulation of next-generation multimode fiber links," *J. Lightw. Technol.*, vol. 21, no. 5, pp. 1242–1255, May 2003.
[24] NRAO, *Very Long Baseline Array Project Book*. VLBA Project Office, 1988.

Jacopo Nanni was born in Bologna, Italy, in 1990. He received the B.Sc and M.Sc degrees in Telecommunications Engineering from University of Bologna in October 2012 and March 2015, respectively. From April to October 2015 he was in University of Bologna as research fellow at the Department of Electrical, Electronic and Information Engineering (DEI) "Guglielmo Marconi", working about low cost and low consumption VCSEL-based Radio-over-Fiber systems for signal distribution in indoor and Radio Astronomy applications. Since November 2015 he has been working in microwave photonics domain as Ph.D. student jointly at University of Bologna, Italy, and at Université Paris-Est, ESYCOM, ESIEE Paris, UPEM in Noisy-le-Grand, France.

Simone Rusticelli obtained the B.Sc degree in Telecommunications Engineering from the Engineering School of the University of Bologna in 2012. His thesis was about the measurement and characterization of devices using RFoF technique for radioastronomic applications with Prof. Giovanni Tartarini. He obtained a two-year (2013-2015) scholarship at the Engineering School of Bologna, studying the possibility of decreasing costs using VCSELs for radioastronomical applications and analyzing gain fluctuation problems in analog single-mode fibre systems. He obtained a scholarship at the National Institute of Astrophysics in Bologna (2015-2016) with the aim of developing LNA and RFoF-based receivers for the Low Frequency Aperture Array, as a part of the Square Kilometre Array (SKA); furthermore the possibility to use high power lasers to feed remote antennas front-end.

Carlos Viana was born in Viana do Castelo, Portugal, in 1986. He received the M.S. degree in Electrical and Computers Engineering from the Faculty of Engineering of the University of Porto (FEUP), Porto, Portugal in 2010 and Ph.D. degree in Electronics, Optoelectronics and Systems from Université Paris-Est, Champs-sur-Marne, France, in 2014. Since 2010 he has been a researcher with ESYCOM laboratory at ESIEE-Paris, Noisy-le-Grand, France. His research interest includes optoelectronics devices developments, integration and packaging for low cost Radio-over-Fiber technology applications.

Jean-Luc Polleux received a Master degree / Diplôme d' ingénieur in microelectronic from ENSEIRB, Bordeaux, France, and the DEA degree in electronic and telecommunications from the University of Bordeaux 1, France, both in 1997. He received the Ph.D. degree in the opto-microwave field from CNAM, Paris, in 2001. He then joined ESIEE-Paris at Université Paris-Est (UPE), France, and the joint laboratory ESYCOM. He is now associate professor. His current research involves microwave-photonics devices and systems for Radio-over-Fibre applications with special emphasis on microwave phototransistors (SiGe/Si and InGaAs/InP), Silicon-based integration and packaging, analogue VCSELs and opto-microwave devices modelling. He published over 90 scientific publications. He co-organized three international workshops, co-chaired the French National Microwave Conference, JNM, in 2013, and chaired and co-chaired the Career Platform of EuMW in 2015 and 2016. He was a guest editor of the International Journal of Microwave and Wireless Technologies (IJMWT) in February 2014. He is coordinating the Institute DIAMON, a Paris Region French Cluster of Research, from 2015, and is an administrator of Optics' Valley cluster.

Catherine Algani received, from the University of Paris 6, France, the DEA degree in Electronics, and the PhD degree, respectively in 1987 and 1990. Her dissertation concerns the area of active MMIC design using GaAs HBTs technology in CNET-Bagneux. In 1991, she joined the electronics engineering department and the LISIF Laboratory, at University of Paris 6, as a lecturer. From 1991 to 2005, she worked on the design of microwave and millimetre-wave integrated circuits on different GaAs technologies. In 1997, she began to work in the area of microwave photonics (optically controlled microwave switches on GaAs and electro-optic organic modulator). In 2005, she joined ESYCOM at Le CNAM in Paris, where she is currently a full professor. Her current research interests are the development of devices, circuits, and sub-systems for ultrahigh speed digital and analog communications for ROF and wireless applications. These researches include the modelling, the design and the characterization of such structures.

Federico Perini (Bologna, Italy, 1974) received the Laurea degree in telecommunications engineering (summa cum laude) from the University of Bologna in 2001. From 2002 he has always worked for IRA (Institute of Radio Astronomy) of INAF (National Institute for Astrophysics) at the Medicina radio telescopes as RF project engineer. His activities are focused on the design and develop of RF/IF receivers and signal transportation systems based on RFoF technology for both the Italian radio telescopes and for the low frequency instrument of the future Square Kilometre Array (SKA).

Giovanni Tartarini is Associate Professor of Electromagnetic fields at the Department of Electrical, Electronic and Information Engineering (DEI) of the University of Bologna. His research interests are in the area of Microwave Photonics, including Radio over Fiber systems and devices for telecommunications (outdoor and in-building wireless signal distribution) and sensing (Radio-Astronomic and UWB signal transmission). He collaborates on these topics with private companies and research institutions. From 2008 to 2011, he was responsible for the University of Bologna of the integrated project “Architectures for Flexible Photonic Home and Access Networks” (ALPHA), sponsored by the European Community in the VII Research Framework Program. Since 2013 he is the responsible of a collaboration with the Italian Institute of Astrophysics for the development and characterization of the Radio over Fiber link of the receiver within the International Radio-Astronomy Project named “Square Kilometer Array” (SKA).